OPEN

Surgical Transcanal Procedure for Injection of Cells and Substances into the Human Cochlear Modiolus

*Per Cayé-Thomasen, †Peter Erfurt, †Peter Baumhoff, †Andrej Kral, and ‡Charlotte Amalie Navntoft

*Department of Otorhinolaryngology, Head and Neck Surgery and Audiology, Rigshospitalet, Copenhagen University Hospital, Copenhagen, Denmark; †Department of Experimental Otology and Institute of AudioNeuroTechnology, Clinics of Otolaryngology, Head and Neck Surgery, Hannover Medical School, Hannover, Germany; and ‡Eriksholm Research Centre, Oticon A/S, Denmark

Introduction: Cochlear implants (CIs) enhance hearing by stimulating spiral ganglion neurons (SGNs) but are less effective in individuals with compromised SGN functionality. Advances in regenerative medicine suggest that local delivery of medical drugs or cell therapy could regenerate the auditory nerve. This study evaluates a minimally invasive technique for precise delivery of cell-sized beads, simulating cell therapy, into the cochlear modiolus of human temporal bones.
Methods: Ten fresh-frozen human temporal bone specimens were used. Five bones served to establish the injection trajectory using a tungsten rod probe, and the remaining five for injecting microbeads into the modiolus. The surgical procedure involved accessing the middle ear via the external ear canal, performing a cochleostomy at the first cochlear turn, and drilling into the modiolus. Beads were injected into the modiolus using a Hamilton syringe connected to an injection pump, followed by micro-computed tomography imaging and histological assessment.
Results: Accurate placement of the tungsten rod probe within the modiolus was achieved in four out of five bones. Microbead injections indicated 89 to 97% retention within the modiolus, with minimal leakage. The technique showed consistent trajectory with low variability.
Conclusion: The study demonstrates the feasibility of a minimally invasive, precise injection method for delivering and retaining cell-sized beads into the cochlear modiolus. This technique enables future local delivery of medical drugs or cell therapy drugs aimed at hearing restoration, benefiting both current CI users and CI candidates. Further research is necessary to evaluate precision, reproducibility, and long-term outcomes of the procedure.
Key Words: Cell therapy—Inner ear surgery—Method development—Modiolar injection—Route of administration—Temporal bone—Transcanal access.

Otol Neurotol **46:**476–484, 2025.

INTRODUCTION

Partial restoration of hearing can be achieved in severe-to-profound hearing-impaired patients by direct electric stimulation of spiral ganglion neurons (SGNs) using a cochlear implant (CI), thereby circumventing the impact of hair cell loss. However, effectiveness of a CI depends on the presence and functionality of SGNs, implying that individuals with limited or absent SGN numbers or function will not benefit fully from an implant. Today, this subgroup of existing CI users and potential CI candidates find themselves devoid of alternative options, apart from an auditory brainstem implant.

Recent advances in regenerative medicine have sparked interest in cell-based therapies as a potential breakthrough for treating hearing loss. Stem cells, with their capacity for self-renewal and differentiation into various cell types, hold promise for regenerating auditory tissue, including SGNs. For instance, Chen et al. (1) transplanted otic progenitor cells derived from human embryonic stem cells (hESC) into the cochlear modiolus of a gerbil model of auditory neuropathy, demonstrating recovered auditory brainstem responses. However, other studies found poor cell survival 1 to 2 weeks after transplantation of murine-derived stem cells into an animal model (2–7). Crucial to success is the ability to deliver the cells safely and precisely to the target structure in the cochlea.

Injection of cells directly into the modiolus, using intramodiolar injections, has been suggested in animal studies (1,2,6) and the technical feasibility has been examined in a couple of cadaveric human temporal bone studies (8–10). A 250- to 300-µl scaffold-based gel with hESCs could be delivered into the internal auditory canal (IAC), creating access via a radical mastoidectomy followed by a cochleostomy in

Address correspondence and reprint requests to: Charlotte Amalie Navntoft, Ph.D., Eriksholm Research Centre, Oticon A/S, Rørtangvej 20, Snekkersten, 3070, Denmark; E-mail: chmv@eriksholm.com
Charlotte Amalie Navntoft, https://orcid.org/0000-0003-0024-6142
Source of Funding: This work was partially supported by Oticon A/S.
Conflicts of Interest: The authors declare no potential conflicts of interest with respect to the research, authorship, and/or publication of this article.
Supplemental digital content is available in the text.

DOI: 10.1097/MAO.0000000000004463

the basal turn immediately anterior–inferior to the round window niche, subsequently breaching the modiolar wall to the IAC (9). Wrobel et al. (10) simulated an intramodiolar injection by inserting a metallic electrode probe into the apical modiolus. This procedure involved accessing the inner ear through the external auditory canal and performing a tympanotomy, followed by a cochleostomy at the end of the second turn, ultimately breaching the modiolar wall. In a related study, Li et al. (8) inserted a metallic probe into Rosenthal's canal in the basal turn via the round window membrane following a mastoidectomy. All these approaches required significant surgical intervention into the temporal bone.

There is still an unmet need for a minimally invasive and precise technique that avoids injection into the IAC (to mitigate the risk of spreading, e.g., otic progenitor cells into the cerebrospinal fluid (CSF) and thus the entire central nervous system (CNS) but allows the injection of a sufficient volume into the modiolus. An optimal approach should also be clinically applicable, fast, and with a low risk of damage to surrounding structures.

In this work, we demonstrate the feasibility of injecting several microliters of cell-sized metal and glass microbeads into the modiolus of the human temporal bone, applying a fast and minimally invasive surgical access from the external auditory canal and a fixed and stable system for control of injection speed and volume. Our findings demonstrate that small beads simulating cells can be accurately targeted to the basal and midmodiolus with minimal tissue damage, as evidenced by reconstructed micro-computed tomography (micro-CT) scans and histological assessment. The approach is compatible with an already implanted CI electrode array, suggesting applicability to both existing CI users and CI candidates.

MATERIALS AND METHODS

Ten fresh-frozen human temporal bone specimens were used for this study. Consistent with the local authorities' ethical rules for handling human tissue, the temporal bones were obtained from donors. The temporal bones were fresh-frozen and for use slowly thawed at room temperature. To establish the injection trajectory, a thin tungsten metal rod probe was inserted into the cochlear modiolus in five temporal bones and the temporal bone underwent scanning to visualize the intended path. Subsequently, based on the trajectory established, small, cell-sized glass or metal microbeads were injected into the cochlear modiolus in five additional temporal bones, in order to establish injection methodology, including aspects of precision and volume.

Transcanal Access to the Modiolus

The preparation of the temporal bone specimens and the surgical approach were performed under a surgical microscope using standard ear surgery instruments.

The middle ear was accessed via the external ear canal. The tympanic membrane was elevated while preserving the ossicular chain. Anatomic landmarks were visualized, including the ossicles, the promontory, the round window niche, and processus cochleariformis, being the same as when finding the scala tympani to place a split CI electrode. The scala tympani at the end of the first cochlear turn was blue-lined immediately anterior to the stapes footplate, immediately inferior to cochleariform process, using a Ø 1.0-mm bur (Medtronic, USA). Drilling was performed until the membranous labyrinth shined through the thinned-out bone, which was removed with a micro pick, allowing access to the tympanic duct of the end of the first cochlear turn, exposing the modiolus. Next, the modiolus was entered and opened by careful drilling at the center of the modiolar wall, just above Rosenthal's canal, creating a round modiolostomy, and subsequently a void within the modiolus, corresponding to the 0.5-mm ball-shaped drill head (Medtronic, USA).

Insertion and Visualization of a Tungsten Metal Rod Probe

To indicate the trajectory path and precision of a simulated intramodiolar injection, the tip of a tungsten rod probe (Tungsten Rod, Ø 127 µm × 76.2 mm, #71600, A-M Systems, USA) was carefully advanced into the modiolus. The probe was fixed using tissue glue (Loctite® 4,161, Henkel, GE), followed by micro-CT imaging of the temporal bone (Zeiss Xradia 480 Versa, Carl Zeiss X-ray Microscopy Inc., Germany; output 80 kV, 9,000 ms exposure, voxel edge length 19 µm).

Injection and Visualization of Cell-Sized Microbeads in the Modiolus

To simulate an injection of cells, microbeads with a size comparable to cells were injected into the cochlear modiolus. The first two bones were injected with glass beads for training purposes, the following three bones with small stainless steel beads (Ø 41–48 µm, #SSMMS-7.8 41–48 µm, Cospheric, USA). The stainless steel beads were dissolved 3:1 in Hank's balanced salt solution (-Ca^{2+}/-Mg^{2+}) (cat no. 14175-053, Gibco, Thermo Fisher Scientific, USA) containing 0.2% human albumin serum (Recombumin Elite, Albumedix, UK) and vitrogel (VitroGel®, TheWell Bioscience, USA), giving a final concentration of 167 mg beads/ml formulation. The beads were injected using a 10-µl Hamilton syringe (701 RN 10 µl, #7635-1, Hamilton, Romania) with a blunt G24 needle (ga24, PST3, Hamilton, USA), placed in a micromanipulator and coupled to an injection pump (UMP3T-1, World Precision Instruments, USA). A volume of 2 µl was injected at 250 µl/min in the first bone (TB03H R) and a 0.6-µl volume was injected at 100 µl/min in the next two bones (TB04H L, TB05H R). The needle was left in place for 1 to 2 minutes to prevent backflow, whereafter the needle was carefully removed and the modiolar wall opening was manually sealed with Surgicel (Tabotamp, reabsorable haemostyptikum, #1901, Ethicon, Germany) to contain the injected volume within the modiolus. The bones were embedded in resin, see details under *Histological Preparation and Microslicing* below, and subjected to a volume scan in a preclinical, cabinet cone-beam micro-CT (µCT 100, software version 1.2b; Scanco Medical, Switzerland). The scans were conducted with an output of 45 kVp, an exposure time of 3,000 ms (600 µAs), and a voxel edge length of either 16.4 µm (TB03H R, TB04H L, TB05H R) or 24.5 µm (TB01H L, TB02H R).

3D Reconstruction of Micro-CT Imaging for Evaluation of Surgical Access Trajectory Path, Cochleostomy Measures, Precision of Modiolar Access and Modiolar Retainment of Injected Cell-Sized Microbeads

The DICOM images were processed using Amira 3D (v. 2023.2; Thermo Fisher Scientific, FEI SAS, Bordeaux, France). Initially, the DICOM images of TB01H R were transformed to orient the modiolar axis perpendicular to the x-axis of the image stack. Subsequently, all other TB imaging datasets were registered to the same planes, achieving consistent orientation. The transformed datasets were then stored again as DICOM files.

Cochleae and ossicles were segmented and labeled using the segmentation module of Amira 3D. The metal probes and the injected stainless steel beads, identified by the highest white value in volume scan, were segmented separately. Three-dimensional vertex surface representations of the segmentation labels were generated in Amira 3D using the "generate surface" module, applying constrained smoothing to preserve the surface representation of single beads.

All angular, length, and volume measures were extracted in Amira 3D using the measuring tools and the label statistics port. Measures are represented in length, and volume measurements are shown in cubic millimeters, rounded to two decimal places. The number of cochlear turns and angular positions were taken relative to the center of the round window.

To determine a safe approach route for the surgical approach, two sets of four fiducials were established for both the surgical entry point and cochleostomy. The surgical entry point refers to the opening toward the promontory, and the cochleostomy refers to the opening toward the scala tympani. These fiducials were used to determine the width and height of the two fenestrations in a manner that would prevent any damage to the cochlear base. Ellipses were fit through the centers of the fiducials for each set, and their area was calculated (area A = Pi × 1/2 height × 1/2 width).

Stack tools in ImageJ (v. 1.54; NIH, USA) were used to create Z-projections from the transformed DICOM images for figures. In some cases, the "re-slice" tool was used to adjust the projection plane, for example, parallel to the surgical approach. The projections utilized either average intensity or standard deviation of intensity to visualize high-contrast edges.

Histological Preparation and Microslicing

Histological preparation was based on methods described by Sieber et al. (11) to allow qualitative histological visualization of the injected beads and cochlear tissue. After injection of the beads, the temporal bones were placed in a mold and fully immersed in a fixation solution of 4% formalin in phosphate-buffered saline (PBS). Following 72 h of storage, the specimens were rinsed in PBS to remove any residual formalin. Dehydration was carried out in four steps, with sequential immersion in 70, 90, and 100% ethanol, followed by 100% methanol, and with each step for 2 days. To enhance the contrast of soft tissue structure against the embedding epoxy, 0.1% acid fuchsin was added during the ethanol steps. After dehydration, the specimens were dried at room temperature in a fume hood for approximately 1 hour. Subsequently, the specimens were embedded in epoxy resin (SPECI-FIX 40, STRUERS, Denmark) to immobilize and preserve mobile structures within the temporal bone, such as membranes and the ossicular chain, during further processing. To ensure optimal penetration of the epoxy resin into the smaller lumina of the temporal bones, the embedded specimens were placed in a vacuum desiccator. The embedded specimens were then subject to μCT and afterward cured at room temperature for at least 7 days before proceeding with additional processing steps.

Microslicing was conducted through sequential grinding and microscopic documentation of the specimens. Grinding was performed using an AutoMet250 Grinder-Polisher (BUEHLER, Lake Bluff, IL, USA) equipped with silicon carbide grinding paper with a grit size of P800. After each grinding step, the newly exposed layer was documented using a VHX-2000 measurement microscope (KEYENCE Corporation, Osaka, Japan), equipped with a VH-Z20UR zoom lens set to 20× magnification and employing image stitching functionality. The extent of material removal was determined by measuring the height of the remaining overmold using a micrometer gauge.

RESULTS

Surgical Procedure Step-by-Step

The modiolus was exposed in all 10 temporal bones by a cochleostomy into scala tympani at the end of the first cochlear turn via a transcanal approach under microscopic control, using standard ear surgery equipment and small diameter burs (see schematic illustration of the approach in Fig. 1A, B). The temporal bone was positioned corresponding to a standard ear surgery procedure, i.e., with the patient lying on the back and the head turned away to a varying degree, depending on the individual ear canal and middle ear anatomy. After transcanal tympanotomy and tympanic membrane elevation, the cochleostomy was performed immediately anterior to the stapes footplate, immediately inferior to the cochleariform process (Fig. 1C-D), allowed by access between the long process of the incus and the malleus handle. Cochleostomy drilling was performed until the membranous labyrinth shined through the thinned-out bone, which was removed with a micro pick, allowing access to the tympanic duct at the end of the first cochlear turn, exposing the modiolus (FIG. 1E-F). The modiolus was entered and opened by careful drilling at the center of the modiolar wall, just above Rosenthal's canal, creating a round modiolostomy, and subsequently a void within the modiolus, corresponding to the 0.5-mm ball-shaped drill head (FIG. 1G).

Evaluation of the Surgical Access Trajectory Path by 3D Rendered μCT Imaging

To simulate the trajectory and target end point for an intramodiolar injection, the tip of the tungsten rod probe was inserted carefully into the modiolus and fixed with glue, followed by μCT imaging. Imaging showed that the probe tip was in the modiolus in four of the five temporal bones (Table 1). In one case, the probe tip missed the modiolus

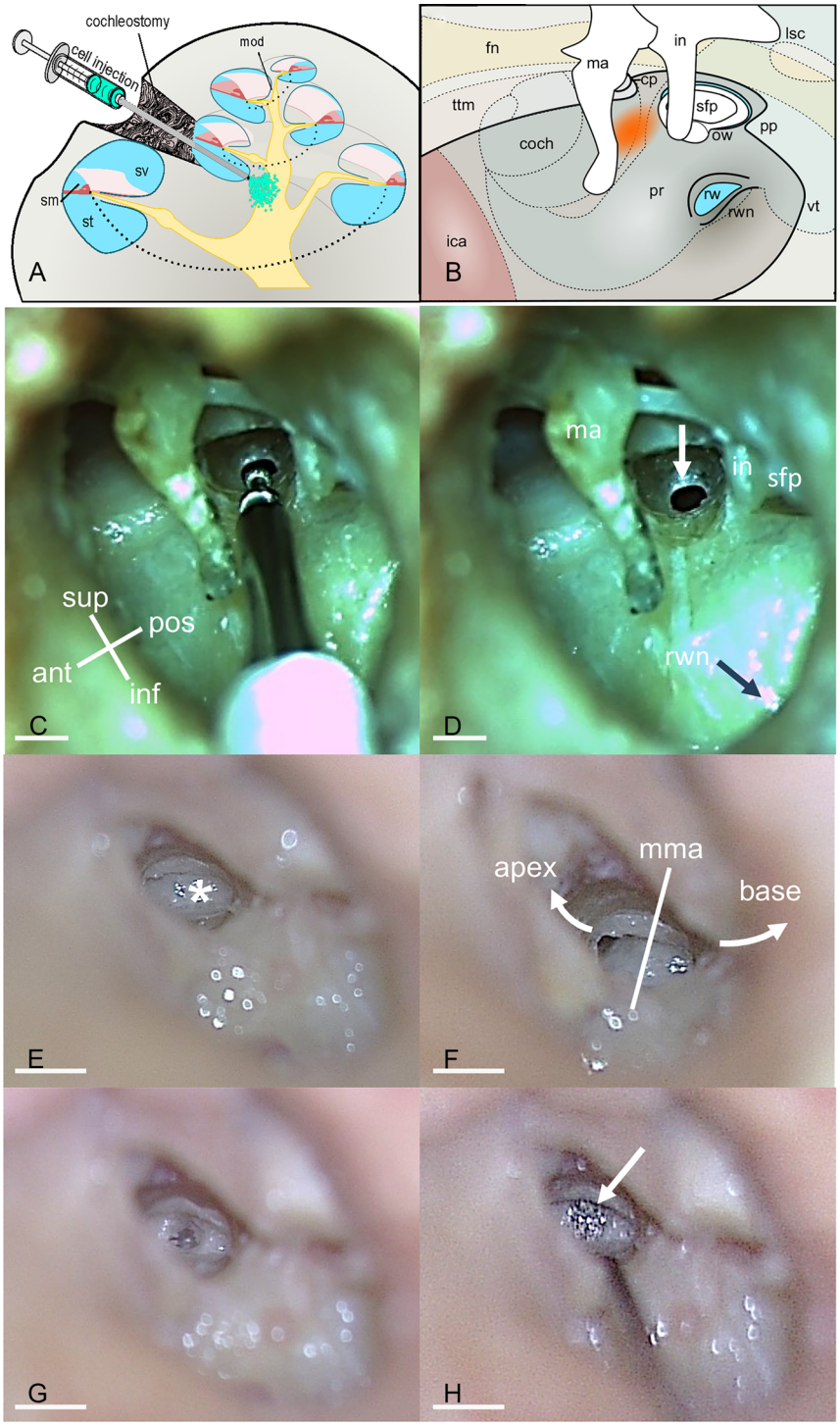

FIG. 1. Illustration and otomicroscopic images of the step-by-step procedure for injecting cells or medical drugs into the modiolus (left ear). *A,* Illustration of the surgical approach showing injection of cells or medicinal drugs (*green*) into the modiolus via access from the end of the first cochlea turn; *B*, illustration of the site of the cochleostomy (*orange*) and anatomical landmarks; *C*, a cochleostomy is performed immediately anterior to the stapes footplate, immediately inferior to the processus cochleariformis, creating a scala tympani opening toward the modiolus at the end of the first cochlear turn; *D*, the cochleostomy (*white arrow*) is approximately 2 mm in diameter. Additional anatomical landmarks are highlighted; *E*, the cribriform modiolar wall is identified (*asterisk*); *F,* when angling the temporal bone somewhat, the path of the scala tympani becomes evident (*dark area to the left and right of the modiolus*). The apex is in the superior–anterior direction; *G,* a Ø 0.5 mm drill is used to gently breach and open the modiolar wall, creating a round modiolostomy; *H,* cell-sized metal microbeads (*arrow*) have been injected into the modiolus using a 24G needle (2 mm scale in *B* and *C*; 1 mm scale in *C*–*F*). Ant indicates anterior; coch, cochlea; cp, cochleariform process; fn, facial nerve; Ica, internal carotid artery; in, incus; inf, inferior; lsc, lateral semicircular canal; ma, malleus; mma, midmodiolar axis; mod, modiolus; ow, oval window; pos, posterior; pp, pyramidal process; pr, promontorium; rw, round window; rwn, round window niche; sfp, stapes footplate; sm, scala media; st, scala tympani; sup, superior; sv, scala vestibuli; ttm, tensor tympani muscle; vt, vestibule.

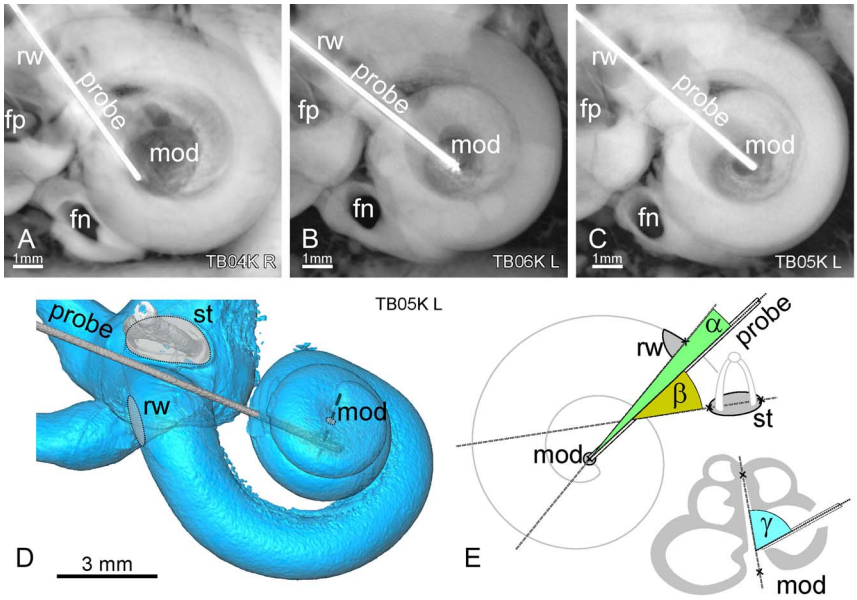

FIG. 2. Surgical trajectory pathway precision and angles demonstrated by insertion of a metal rod probe, illustrated by μCT imaging of three of the temporal bones. *A–C.* μCT images of three representative temporal bones (TB) from a bottom view with the tip of a thin tungsten metal rod probe (*white*) targeted to the modiolar center. *A,* The probe tip in the osseous spiral lamina, missing the target in the modiolus; *B,* the probe tip is in the lateral part of the modiolus, semi on-target in the modiolus; *C,* the probe tip is on-target in the modiolus center; *D.* 3D reconstruction of a temporal bone with insertion of the probe into the modiolus; *E,* a schematic illustration of the various precision and angle measures extracted from the 3D rendered μCT images, including angles of the probe relative to the round window–modiolar axis (*α*), the stapes footplate (*β*), and the midmodiolar axis (*γ*). Results are detailed in Table 1. Fn indicates facial nerve canal; fp, stapes footplate; mod, modiolus; rw, round window.

entirely (Fig. 2A). In two cases, the probe tip was within the modiolus, but not centered optimally (example in Fig. 2B), and in the remaining two cases, the probe tip was located in an optimal position at the center of the modiolus (example in Fig. 2C). 3D reconstruction of a bone with the rod probe tip on-target is shown in Figure 2D. Table 1 shows quantification of the variability of the angle of the surgical trajectory path to the modiolus, based on 3D rendered μCT scans. The insertion point was on average 339.5° (SD ± 8.23°) relative to the round window, corresponding to a location in the end of the first cochlea turn. The probe tip hit the vertical midmodiolar axis on average 72.2° (SD ± 6.3°), implying a trajectory path less than perpendicular to the midmodiolar axis. The relatively low standard variation (SD <7°) in the three angles (α, β, γ) describing the probe trajectory indicates low variability in the procedure and/or that there is limited space to navigate the probe once the modiolus is identified.

Evaluation of the Cochleostomy by 3D Rendered μCT Imaging

To test the feasibility of the injection of cells, microbeads with a size comparable to cells were injected into the cochlear modiolus in five temporal bones. The dimensions of the bones used for insertion of a metal probe (TB04K–TB08K, see above) and for injection of microbeads (TB01H–TB05H) were similar (Supplementary Table 1, http://links.lww.com/MAO/C69; Fig. 3A,B). For the bones injected with beads, the size of the cochleostomy opening toward the tympanic scala amounted to 1.38 mm^2 (SD ± 0.29 mm^2) with a width and height of 1.58 mm (SD ± 0.27) and 1.13 mm

TABLE 1. *Means and variability of surgical trajectory path angles based on 3D rendered μCT scans of the five temporal bones with a metal rod probe inserted into the modiolus*

TB Specimen	Insertion re. rw (°)	α	β	γ	Modiolus Hit? (Y/N)
TB04K R	332.9	−17.4	35.2	74.8	N
TB05K L	353.0	−4.8	30.7	79.8	Y
TB06K L	338.1	−1.5	31.6	76.8	Y
TB07K L	340.5	−2.2	28.1	65.1	Y
TB08K R	333.0	−0.7	29.7	67.1	Y
Mean	339.5 ± 8.23	−5.3 ± 6.9	31.1 ± 2.7	72.7 ± 6.3	

The probe was inserted through a cochleostomy at the end of the first cochlear turn, using a transcanal surgical approach. The three angles are illustrated in Figure 2E. α indicates angle of the probe relative to the round window–modiolar axis; β, angle of the probe relative to the orientation of the stapes footplate; γ, angle of the probe relative to the midmodiolar axis; rw, round window; TB, temporal bone; Y, Yes; N, No.

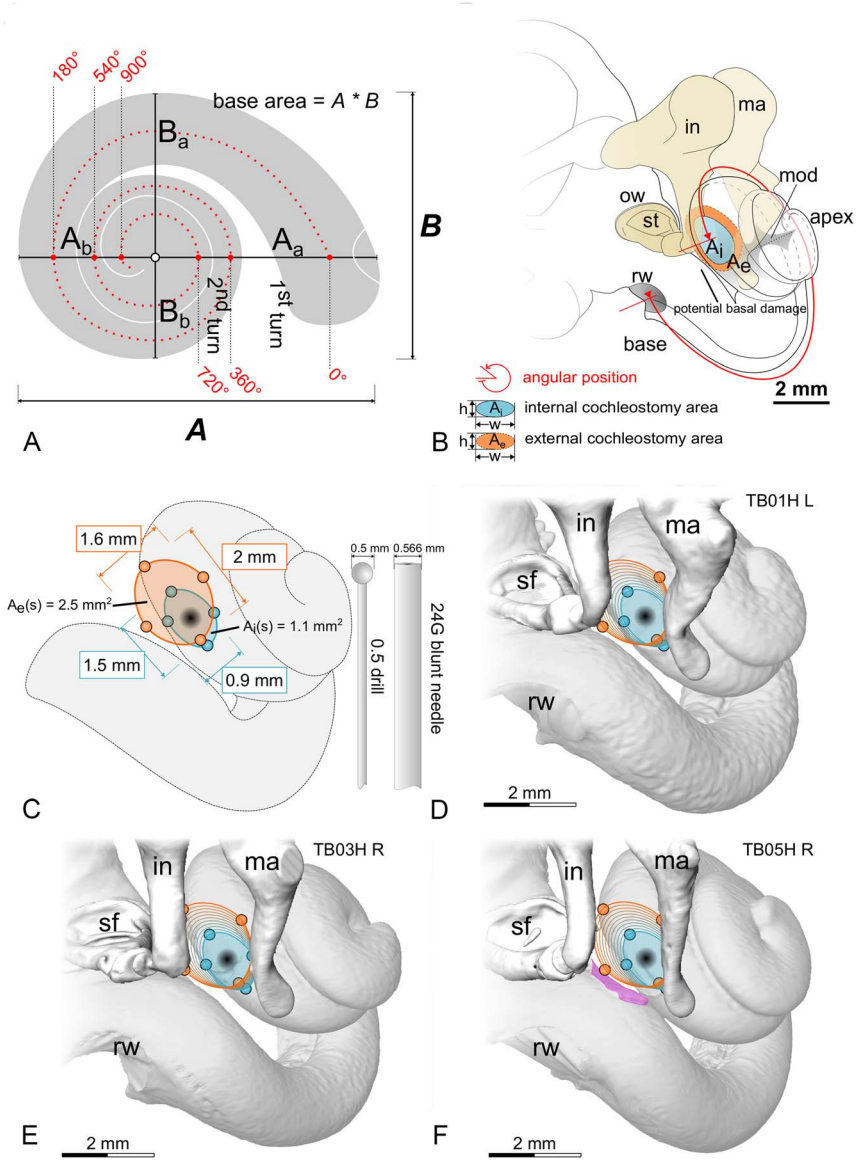

FIG. 3. Illustration of measures of the cochleae and the cochleostomy, and of a safe cochleostomy toward the modiolus. *A,* Measurements encompass the axes A and B (divided into A_a and A_b, as well as B_a and B_b at the modiolus), the base area (A*B), and the number of turns (spiral angle); *B,* schematic of cochleostomy measures in bones injected with microbeads (n = 5). The elliptical area of the drilling entry into the lateral wall of the cochlea from the middle ear (entry point area, A_e, *orange*) is defined by maximal height and width of the external bone opening. The elliptical cochleostomy area (A_i, *blue*) is defined by the maximal height and width of the entry into the scala tympani, and the angular position of the center of the cochleostomy measured from the center of the round window (*red line*). The area at the basal turn, prone to potential damage during drilling, is marked in pink; *C,* eight fiducial points were placed to mark maximum height and width of the lateral cochlear wall drilling entry point from the middle ear (*orange*) and the cochleostomy toward the scala tympani (*blue*), to delineate a safe surgical access route toward the modiolus. A 0.5 ball tip drill and a 24G blunt needle are shown for size comparison; *D–F,* examples of three temporal bones shown as 3D segmentations of the cochlea and the ossicular chain with the drilling entry point (*orange*) and cochleostomy opening (*blue*). Note that unintentional drilling damage may occur toward the scala vestibuli of the basal turn (*pink*) in *F.* $A_{i(s)}$ indicates safe area for cochleostomy; $A_{e(s)}$, safe area for entry point; in, incus; ma, malleus; mod, modiolus; ow, oval window; rw, round window; st, stapes.

(SD ± 0.23 mm), respectively (Table 2). The cochleostomy was not quantified in the bones with the probe inserted due to the large artifact from the electrode probe, which hindered precise measurements.

The area of the surgical entry point from the middle ear (A_e) and the cochleostomy towards the tympanic scale (A_i) was enlarged in the last two bones (TB04H L, TB05H R) to improve visualization of the injection site during the microbead injection. This inadvertently introduced a perforation into the scala vestibuli, causing damage to the basal turn (avoidance of this was not the focus) (Table 2, *appointed area* in Fig. 3B).

To prevent such damage, eight points were established based on measures in Table 2, to determine the height and width of both entry point and cochleostomy, defining a safe surgical access route through the temporal bone. These

TABLE 2. *Measures of the external cochleostomy surface area (entry from the middle ear) and internal cochleostomy surface area (opening into the tympanic scale) in the five temporal bones injected with microbeads*

TB Specimen	Entry Height (mm)	Entry Width (mm)	A_e (mm^2)	Coch Center (° re rw)	Coch Width (mm)	Coch Height (mm)	A_c (mm^2)	Basal Turn Damage (Y/N)
TB01H L	1.77	2.45	3.41	338.7	1.73	0.9	1.22	N
TB02H R	1.59	2.24	2.80	344.1	1.75	0.85	1.17	N
TB03H R	1.67	1.75	2.30	332.5	1.12	1.3	1.14	N
TB04H L	2.12	2.27	3.78	340.8	1.58	1.25	1.55	Y
TB05H R	2.33	2.50	4.57	338.3	1.72	1.34	1.81	Y
Mean ± SD	1.9 ± 0.32	2.44 ± 0.30	3.37 ± 0.88	338.9 ± 4.2	1.58 ± 0.27	1.13 ± 0.23	1.38 ± 0.29	

The measures are illustrated in Figure 3C. A_e indicates area entry point; A_c, area cochleostomy; coch, cochleostomy; TB, temporal bone; rw, round window.

fiducial markers and the resulting elliptical areas for entry point ($A_{e(s)}$ = 2.5 mm^2) and cochleostomy ($A_{c(s)}$ = 1.1 mm^2) are schematically shown in Figure 3C. Drilling within these areas defined by the fiducial markers would allow modiolar access without causing basal damage in all five specimens. Three representative bones with marked entry point (*orange*) and cochleostomy (*blue*) are displayed for comparison in Figure 3D–F.

Evaluation of the Injection of Cell-Sized Microbeads into the Modiolus

Through the surgical microscope, the first two temporal bones were used to establish the injection protocol using manual injection of the beads into the modiolus. This approach resulted in extensive spill-out of the beads into the scalae (not shown). To prevent the movement of the needle tip and enhance precision, a micropump and micromanipulator was subsequently used to inject the volume. This ensured a stable positioning of the needle at the modiolus, effectively allowing for the injection of an appropriate volume into the modiolus.

The bulk of the injection was clearly visible and single metal beads distinguishable in the histological preparation (Fig. 4A). The high-density metal beads were also detectable on the μCT images in the same specimen (Fig. 4B), allowing segmentation of the beads (Fig. 4C). Worth noting is that apart from the modiolostomy and intended void within the modiolus, the modiolar anatomy remained intact.

The injection technique was progressively optimized across injection of the following three temporal bones (Fig. 4D–F) by adjusting injection volume, injection speed, and placement of the needle, leading to an increased proportion of beads deposited within the modiolus (Fig. 4G).

In the first bone, the needle tip was positioned inside the modiolus, resulting in 53% of the beads located on-target within the modiolus, with a spilling of the remaining beads into the scala tympani and along the surgical path, and some into the IAC (Fig. 4D, G). The volume of beads and injection rate were subsequently reduced to 0.6 μl and 100 μl/min, respectively, with the needle tip positioned not within the modiolus, but at the modiolar wall opening, thus increasing the void in the modiolus to be filled and preventing bead spill-out from back-flush. In the second bone, this adjustment resulted in 89% of the beads being retained on-target within the modiolus, largely avoiding spilling into the scala tympani (Fig. 4E, G). The volume percentage of beads remaining within the modiolus after injection increased further to 97% in the third temporal bone (Fig. 4F,G). In this final specimen, the beads were located at a distance from the IAC.

Overall, the results demonstrate the feasibility of injecting and targeting beads, comparable in size and shape to human stem cell–derived otic progenitor cells, to the human cochlear modiolus with minimal spilling or wash-out. The study provides the detailed method and a proof-of-principle that volumes of at least 0.5 μl can be successfully injected and retained within the human modiolus using this approach.

DISCUSSION

Animal studies injecting cells directly into the modiolus rather than into the perilymph or internal auditory meatus have shown the highest success rate in terms of cell survival, differentiation, and neurite outgrowth (1,2,6,12–18). These findings suggest that delivering cells directly into their target environment is crucial, as this may provide necessary endogenous neurotrophic factors and reduce the need for cell migration.

In this study, we demonstrate proof-of-principle of injecting a small volume of microbeads into the cochlear modiolus of human temporal bones using a transcanal approach. Such an approach is readily familiar to many ear surgeons. Unlike the few previous studies, this approach targets the end of the first cochlear turn and thus the basal and midportion of the modiolus, implicating that low-to-mid frequency hearing is important for speech recognition. The targeted site offers several advantages, including potential for a larger injection volume, a low risk of damage to surrounding structures including the vestibular system, the facial nerve, and chorda tympani, and a safe distance from the IAC to avoid not only leak of CSF, but also spread of injected material to the CSF and further into the CNS. In addition, the transcanal approach is less invasive compared to access via a mastoidectomy. More invasive approaches to access the modiolus, such as removing the cochlear duct to improve visualization for the resection of intralabyrinthine schwannomas followed by cochlear implantation, have shown excellent audiological results in recent studies (19–21). However, our approach prioritizes minimizing damage, both as a general principle and due to the heightened sensitivity of the patient group to factors such as compromised vascular supply and unwanted tissue response, which are of particular importance in the context of cell transplantation. Finally, the approach may also be applicable to existing CI users with standard electrode arrays, as the tip of the electrode is basal to the cochleostomy and modiolar entry in most cases, although this remains to be explored. If

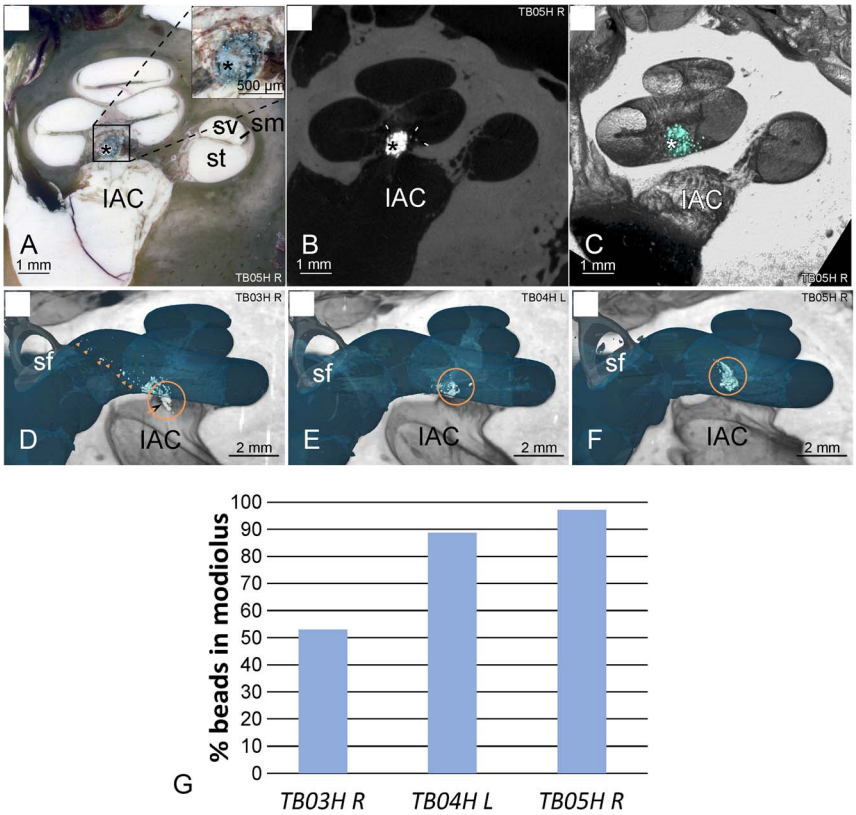

FIG. 4. Visualization of the metallic microbeads injected into the modiolus. *A,* Histologic image of a midmodiolar section of a micropolished resin-embedded temporal bone specimen. The bulk of the injection is clearly visible within the modiolus (*asterisk*) and individual beads are distinguishable (see inset for larger scale); *B*, the high-density metal beads are clearly detectable in µCT imaging of the same specimen shown in *A*; *C*, illustration of the volume segmentation of the injected beads (mint) based on 3D rendered µCT images (same temporal bone as shown in *A* and *B*). *D–F*. 3D reconstructions of the three temporal bones injected with metal microbeads. Most of the beads are in the modiolus (*orange circles*), but some are not (see *G*). Note that some beads located unintentionally in the IAC in *D* (*arrow*), while the beads are located almost entirely within the modiolus and at a safe distance from the IAC in *F*; *G*, proportion of cell-sized microbeads contained on-target within the modiolus relative to the injected volume in the three successive temporal bones injected with metal beads, demonstrating a learning curve and achievement of nearly complete modiolar containment of the injected volume in the last specimen (*right*). The proportion calculations were based on volume segmentation of the 3D rendered µCT images illustrated in *D–F*. IAC indicates internal auditory canal; sf, stapes footplate; sm, scala media; st, scala tympany; sv, scala vestibuli.

the tip of an electrode is visualized in the tympanic scale upon cochleostomy, conceivably, the electrode could be retracted slightly before entering and injecting the modiolus and repositioned thereafter.

Targeted cochleostomies of the first or second turn have been described for the implantation of single or double CI electrodes in the ossified cochlea. However, these procedures were typically performed transmastoidally, often involving partial removal of the osscicular chain (22–24). In contrast, the current approach preserves the ossicular chain. The cochleostomy was sized to provide adequate space for identifying, carefully drilling, and injecting material in a controlled way into the modiolus. With further surgical training and procedure refinement, the cochleostomy size can probably be reduced, thereby also minimizing the risk of entering the basal turn unintentionally.

A thin tungsten rod probe was inserted into the cochlear modiolus to demonstrate and evaluate the precision and variability of the surgical trajectory path on 3D rendered µCT images. Then, cell-sized glass or metal microbeads were injected into the modiolus to demonstrate the feasibility of an intramodiolar injection. To our knowledge, this study is the first to use beads mimicking cells, allowing not only evaluation and quantification of the surgical access by a combination of µCT and histology, but also precise localization of the injected beads and quantification of the proportion of the injected volume contained within the cochlear modiolus. Microbead injections demonstrated retention rates of 89 to 97% within the modiolus, indicating that a substantial portion of future injected cells can be targeted and retained in this structure.

In this study, several important lessons were learned: (i) It is crucial to ensure that the injection is not too basal to avoid entering the IAC. This can be achieved by using a trajectory at a less acute angle to the midmodiolar axis. (ii) One can minimize backflow and spill-out of injected material by utilizing a micromanipulator and injection pump, which allows for precise control and stability of the injection process, including control of injection speed and volume. The present experiments demonstrate that volumes of 0.6 µl can be safely injected using this procedure if injected at a slow speed (100 µl/min). The micromanipulator in combination with

the injection pump eliminate micromovements that are unavoidable when using manual control only. (iii) Damage, in the form of a perforation into the scala tympani of the basal turn, was observed in two out of five bones injected with beads. As the focus of the present experiments was on injecting the modiolus at the end of the first turn, we believe that this risk can be eliminated with the suggested trajectory combined with increased awareness and practice.

Future Directions

In future research, several avenues warrant exploration to further enhance the clinical applicability of the intramodiolar approach for local delivery of cell and drug therapy. Firstly, more experiments on temporal bones injected with microbeads are needed to strengthen the evaluation of precision, as well as the reproducibility and variability of the approach, including the distribution and modiolar containment of the beads. Moreover, potential damage to blood vessels caused by the procedure needs investigation. Utilizing advanced image-guided surgery techniques may help in visualizing and minimizing risks, ensuring the safety of the injection method. Moreover, it is well known that a cochleostomy can induce the formation of fibrous tissue and new bone at the site of intervention (25). This inflammatory response could potentially impact the survival and engraftment of transplanted cells and/or the efficacy of an injected drug. Therefore, it is important to explore how this response affects transplanted cells and/or drug diffusion, to develop strategies to mitigate any negative impacts. This could involve using local or systemic anti-inflammatory treatment or modifying the surgical technique to reduce tissue trauma.

One limitation of the study is that it was conducted on dead tissue, which may absorb fluids and materials differently than living tissue. Therefore, the effectiveness and potential complications of the technique need further investigation in vivo. Future studies should include late preclinical studies in large animals or nonhuman primates, as their cochlear anatomy is similar to that of humans.

Finally, assessing the feasibility of this procedure in patients with an already implanted electrode array remains to be explored. Such evaluation will help determine if any modifications are needed to accommodate the presence of the electrode array, or whether the injection technique is only applicable in existing CI users with electrode arrays shorter than an insertion angle of around 340° (Table 2), which is the target site for the cochleostomy in the end of the first turn.

CONCLUSION

We hereby demonstrate the feasibility of a minimally invasive, transcanal surgical approach for therapeutical injection into the modiolus of the human cochlea, paving the way for future local delivery of, e.g., cell therapy or medical drugs.

REFERENCES

1. Chen W, Jongkamonwiwat N, Abbas L, et al. Restoration of auditory evoked responses by human ES-cell–derived otic progenitors. *Nature* 2012;490:278–82.
2. Corrales CE, Pan L, Li H, et al. Engraftment and differentiation of embryonic stem cell–derived neural progenitor cells in the cochlear nerve trunk: growth of processes into the organ of corti. *J Neurobiol* 2006;66:1489–500.
3. He Y, Zhang PZ, Sun D, et al. Wnt1 from cochlear Schwann cells enhances neuronal differentiation of transplanted neural stem cells in a rat spiral ganglion neuron degeneration model. *Cell Transplant* 2014;23:747–60.
4. Hu Z, Wei D, Johansson CB, et al. Survival and neural differentiation of adult neural stem cells transplanted into the mature inner ear. *Exp Cell Res* 2005;302:40–7.
5. Ishikawa M, Ohnishi H, Skerleva D, et al. Transplantation of neurons derived from human iPS cells cultured on collagen matrix into guinea-pig cochleae. *J Tissue Eng Regen Med* 2017;11:1766–78.
6. Lang H, Schulte BA, Goddard JC, et al. Transplantation of mouse embryonic stem cells into the cochlea of an auditory-neuropathy animal model: effects of timing after injury. *J Assoc Res Otolaryngol* 2008;9:225–40.
7. Nayagam BA, Backhouse SS, Cimenkaya C, Shepherd RK. Hydrogel limits stem cell dispersal in the deaf cochlea: implications for cochlear implants. *J Neural Eng* 2012;9:065001.
8. Li H, Agrawal S, Rohani SA, et al. Unlocking the human inner ear for therapeutic intervention. *Sci Rep* 2022;12:18508.
9. Matsuoka AJ, Sayed ZA, Stephanopoulos N, et al. Creating a stem cell niche in the inner ear using self-assembling peptide amphiphiles. *PLoS ONE* 2017;12:e0190150.
10. Wrobel C, Bevis NF, Meyer AC, Beutner D. Access to the apical cochlear modiolus for possible stem cell-based and gene therapy of the auditory nerve. *Otol Neurotol* 2021;42:e371–7.
11. Sieber D, Erfurt P, John S, et al. The OpenEar library of 3D models of the human temporal bone based on computed tomography and microslicing. *Sci Data* 2019;6:180297.
12. Coleman B, Hardman J, Coco A, et al. Fate of embryonic stem cells transplanted into the deafened mammalian cochlea. *Cell Transplant* 2006;15:369–80.
13. Hu Z, Ulfendahl M, Petri Olivius N. NGF stimulates extensive neurite outgrowth from implanted dorsal root ganglion neurons following transplantation into the adult rat inner ear. *Neurobiol Dis* 2005;18:184–92.
14. Iguchi F, Nakagawa T, Tateya I, et al. Trophic support of mouse inner ear by neural stem cell transplantation: *NeuroReport* 2003;14:77–80.
15. Ogita H, Nakagawa T, Lee KY, et al. Surgical invasiveness of cell transplantation into the guinea pig cochlear modiolus. *ORL J Otorhinolaryngol Relat Spec* 2009;71:32–9.
16. Okano T, Nakagawa T, Endo T, et al. Engraftment of embryonic stem cell–derived neurons into the cochlear modiolus. *Neuroreport* 2005; 16:1919–22.
17. Sekiya T, Holley MC, Hashido K, et al. Cells transplanted onto the surface of the glial scar reveal hidden potential for functional neural regeneration. *Proc Natl Acad Sci U S A* 2015;112:E3431–40.
18. Shi F, Corrales CE, Liberman MC, Edge ASB. BMP4 induction of sensory neurons from human embryonic stem cells and reinnervation of sensory epithelium. *Eur J Neurosci* 2007;26:3016–23.
19. Nassiri AM, Staricha K, Neff BA, et al. Cochlear implantation outcomes in patients with sporadic inner ear schwannomas with and without simultaneous tumor resection. *Otol Neurotol* 2024;45:1051–4.
20. Iannacone FP, Rahne T, Zanoletti E, Plontke SK. Cochlear implantation in patients with inner ear schwannomas: a systematic review and meta-analysis of audiological outcomes. *Eur Arch Otorhinolaryngol* 2024; 281:6175–86.
21. Plontke SK, Iannacone FP, Siebolts U, et al. A case report demonstrating preservation of vestibular receptor function after transcochlear removal of an intracochlear schwannoma with extension to the fundus of the internal auditory canal. *J Clin Med* 2024;13:3373.
22. Isaacson B, Roland PS, Wright CG. Anatomy of the middle-turn cochleostomy. *Laryngoscope* 2008;118:2200–4.
23. Lenarz T, Battmer RD, Lesinski A, Parker J. Nucleus double electrode array: a new approach for ossified cochleae. *Otol Neurotol* 1997;18(6 Suppl):S39–41.
24. Vashishth A, Fulcheri A, Prasad SC, et al. Cochlear implantation in cochlear ossification: retrospective review of etiologies, surgical considerations, and auditory outcomes. *Otol Neurotol* 2018;39:17–28.
25. Somdas MA, Li PMMC, Whiten DM, Eddington DK, Nadol JB Jr. Quantitative evaluation of new bone and fibrous tissue in the cochlea following cochlear implantation in the human. *Audiol Neurootol* 2007; 12:277–84.